Available online at www.sciencedirect.com

SCIENCE DIRECT®

Optics Communications 226 (2003) 81–88

OPTICS COMMUNICATIONS

www.elsevier.com/locate/optcom

An antireflective silicon grating working in the resonance domain for the near infrared spectral region

L. Escoubas [a,*], J.J. Simon [a], M. Loli [a], G. Berginc [b], F. Flory [a], H. Giovannini [a]

[a] *Institut Fresnel – Unité Mixte de Recherche 6133, Centre National de la Recherche Scientifique,*
Ecole Nationale Supérieure de Physique de Marseille, 13397 Marseille cedex 20, France
[b] *Thalès Optronique, Rue Guynemer – BP55, 78283 Guyancourt cedex, France*

Received 12 April 2003; received in revised form 23 July 2003; accepted 31 August 2003

Abstract

We have designed and fabricated a silicon grating which shows antireflection properties, in normal incidence, in the [4μm; 6μm] spectral region. This configuration is of utmost importance for stealth applications when laser telemeters are used to localize moving targets. It is shown that although the grating parameters are outside the validity domain of diffraction homogenization theories, the opto-geometrical parameters given by the effective medium theory can be used as starting solutions for designing the structure. This allows the use of a standard low-resolution etching technique for fabricating the grating. The reflectance is calculated with a modal method and compared successfully with the experimental results. It is shown that the grating reduces the silicon substrate reflectance in the whole [4μm; 6μm] spectral domain by a factor greater than 10.

PACS: 42.79.D; 42.79.W; 42.70.K; 81.65.C

Keywords: Antireflection surfaces; Diffraction gratings; Infrared; Homogenization theory; Effective medium theory; Modal method; Wet anisotropic etching

---

1. Introduction

Coating is the standard way of reducing reflection on optical surfaces. However, in certain cases, alternative solutions are required. For infrared applications, for example, the thickness of the deposited layers is of the order of few micrometers. Such thick coatings exhibit stress which may induce poor surface adhesion which is of a crucial importance, especially for aerospace applications where optical components have to resist strong temperature variations and strong velocity accelerations. Moreover, the performances of thick coatings can also be affected by absorption. Sub-wavelength grating structures turn out to be a low cost highly effective alternative way of reducing reflection [1,2]. Such antireflection corrugated

---

[*] Corresponding author. Tel.: +33-4-91-28-80-68; fax: +33-4-91-28-80-67.

E-mail address: ludovic.escoubas@fresnel.fr (L. Escoubas).

0030-4018/$ - see front matter © 2003 Elsevier B.V. All rights reserved.
doi:10.1016/j.optcom.2003.08.034

surfaces made on lossy materials such as semiconductors and metals have proved useful for eliminating specular reflection, in particular for visible light [3]. Surface-relief grating structures made on semiconductor materials have also been used to increase the efficiency of solar cells [4]. Gold surface-relief rectangular-groove gratings have also been designed and fabricated to be antireflecting [5].

When the incident medium is air, in normal incidence, and when the grating period is much smaller than the wavelength, only the zeroth order is reflected and the corrugated layer acts as an effective medium covering a homogeneous substrate [6,7]. In this case, sub-wavelength gratings can mimic the effects of thin-film coatings. Homogenization theories [8] have demonstrated that the surface acts as a graded index layer whose permittivity along z-axis (see Fig. 1) depends on the filling factor f. Due to the pyramidal profile of the grating considered in this paper, the filling factor is a function of z. At each value of $z > 0$, the effective index of the corrugated surface is a combination of the indices of the substrate and of the incident medium. Several studies have been conducted to optimize the profile of the grating in order to obtain the lowest reflectance [9,10]. Given that, to be valid, homogenization theories need the grating period to be much smaller than the wavelength. Thus, designing and fabricating antireflection corrugated surfaces working in the near infrared usually need micrometric resolution etching techniques.

In this paper, our objective is to design and to manufacture bi-dimensional gratings that can be used to reduce the reflectance of infrared detectors. This problem is of utmost importance for stealth applications when laser telemeters are used to detect and to localize moving targets. We show that, as already predicted by other authors [1], a corrugated surface reduces the reflection as long as there are no resonance and no blazing. More precisely, we demonstrate that a strong antireflection effect can be obtained in certain cases even when the optogeometrical parameters of the gratings are outside the domain of validity of homogenization theories. We show, both theoretically and experimentally, that the reflectance of a silicon substrate can be reduced by a factor greater than 10 in normal incidence with a grating whose period is close to the wavelength of illumination. This result is of practical interest for stealth applications as it demonstrates that high-resolution etching techniques are not required for fabricating antireflection structures working in the near infrared. We apply our results to the design and to the fabrication of a bi-dimensional antireflection grating working in the [4μm; 6μm] spectral region. The sample, which is a pyramid-shaped silicon grating, has been fabricated using photolithography and silicon chemical etching techniques. The microstructure morphology of the sample has been characterized by optical interferometric microscopy and atomic force microscopy. The reflectance has been measured by standard spectrophotometric techniques. The measured reflectance is less than 2.5% in the 4–6 μm range.

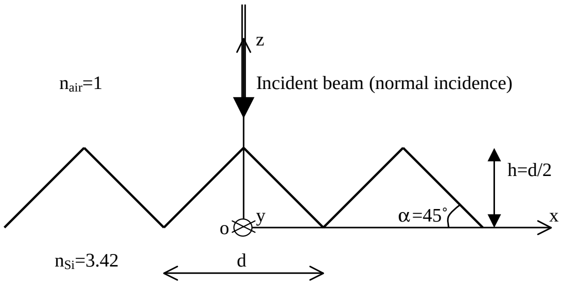

Fig. 1. xoz section of the 3D pyramidal profile of the bi-dimensional grating.

In Section 2, we briefly describe the calculation method used for the numerical simulations and we present the steps that led to the geometry of the proposed structure. Section 3 describes the etching process. In Section 4, we present our experimental results. We compare the spectral response of the grating with that obtained numerically. A comparison is drawn between the antireflection effect obtained with our structure and that obtained with standard thin film coatings.

2. Theory and simulation

The gratings considered in this paper are bi-dimensional, made of silicon whose refractive index n_{Si} is equal to 3.42 in the spectral region

[4 μm; 6μm]. For such a value of n_{Si}, the reflectance defined on the intensity, for a plane surface, is around 30% at normal incidence. The grating period and its thickness are close to the wavelength of illumination. These parameters are such that, in order to calculate the amount of diffracted light from the grating structure, a computer code based on a rigorous method of calculation must be used. However, in order to avoid the use of optimization methods that require time and memory consuming calculations, we first calculated the reflectance of the gratings using a first-order effective medium theory. In this case, the effective permittivity at height z (see Fig. 1) is equal to the average permittivity of the bi-dimensional structure calculated in a plane parallel to the plane (xoy). We used this method to determine the period and the depth of an antireflection structure that was our starting solution for designing the grating's surface. As etching was made on a $\{1\,0\,0\}$ silicon wafer, we considered, for the corrugated surface, an inclination angle of 45° corresponding to $\{1\,1\,0\}$ planes of silicon (see Fig. 1). This particular etching leads to pyramid-shaped gratings. As this value could easily be obtained with our photolithography technique (see Section 3), the grating period d was chosen to be greater than 3 μm. For pyramid-shaped gratings with an inclination angle $\alpha = 45°$, the effective index n_{eff} of the layer varies from the value $n_{\mathrm{eff}} = n_{\mathrm{Si}} = 3.42$ of silicon at height $z = 0$ to the value $n_{\mathrm{eff}} = n_{\mathrm{air}} = 1$ at height $z = h = d/2$ as a function of z, with

$$n_{\mathrm{eff}} = \left(1 + \frac{n_{\mathrm{Si}}^2 - 1}{h^2}(h - z)^2\right)^{1/2}. \qquad (1)$$

The height h of the structure has been determined in order to obtain a strong antireflection effect. The value $h = 2.5$ μm leading to a period $d = 5$ μm has been reached. Fig. 2 shows the calculated reflectance of a graded index layer on a silicon wafer. A strong reduction of the reflectance, which remains smaller than 2.2% in the whole spectral domain, is obtained with the graded index layer. In order to predict, without approximation, the behavior of the grating whose profile is shown in

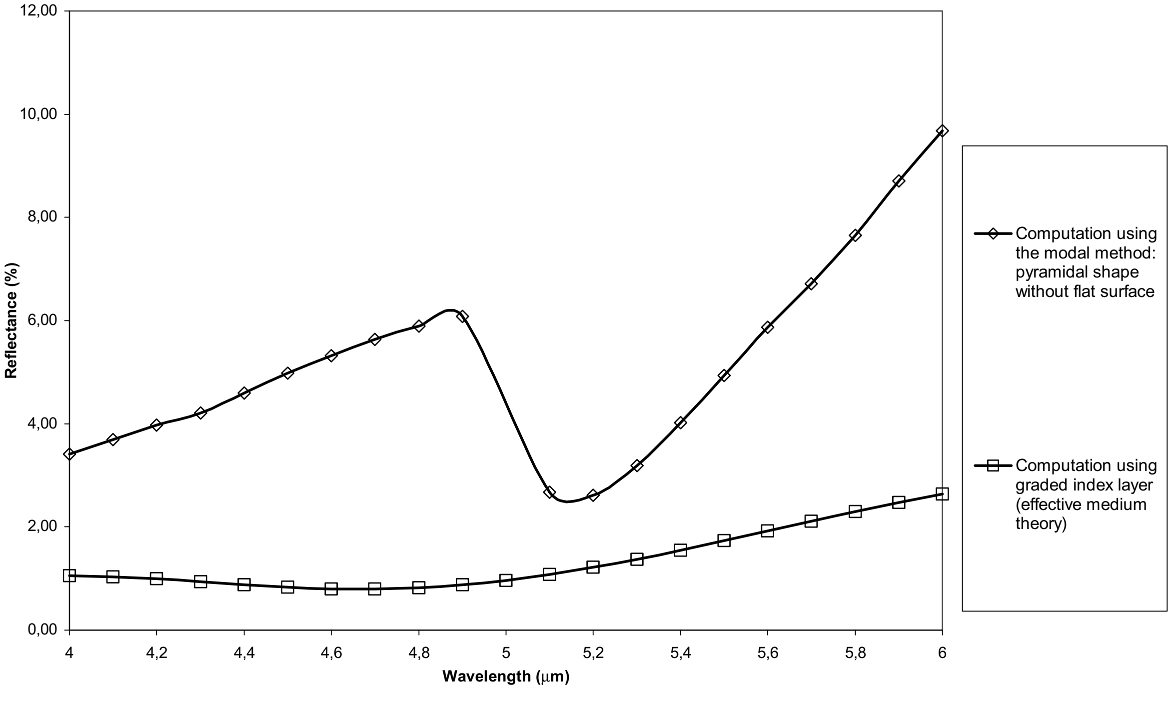

Fig. 2. Reflectance of the structure calculated by using the effective medium theory and the modal method (normal incidence).

Fig. 1, we used a 2D computer code based on a vector modal method [11] with 17 coefficients for both directions, that is 289 coefficients for the bi-dimensional grating. The number of coefficients guarantees accuracy better than 1% for the gratings considered in this paper. The computed reflectance is shown in Fig. 2. The kink around 5 μm on the curve obtained with the modal method corresponds to the disappearance of $[1,0]$, $[0,1]$, $[-1,0]$ and $[0,-1]$ orders. It can be seen that, as expected, the result differs from the one given by the effective medium theory. However the value of the reflectance remains smaller than 10% in the whole spectral domain. In this case, the reflectance of the silicon wafer is reduced by a factor of 3. For this reason, we decided to fabricate and to characterize the bi-dimensional grating whose profile is represented in Fig. 1.

3. Process

3.1. Wet anisotropic etching of silicon

In microtechnology, wet anisotropic etching is a common technique used to create 3D structures in the bulk of crystalline silicon wafers [12]. This technique uses a mask pattern in order to protect silicon surface zones from etching, whereas exposed silicon zones are dissolved in the etchant [13–20]. In other wet etching processes, photoresist is often the chosen masking layer. But, in the case of wet anisotropic etching of silicon, a thermal silicon oxide layer (referred to as a hard mask) is often grown and used as an appropriate mask against etching. Indeed, the wet etchant is very selective to silicon compared to silicon oxide. In the case of crystalline silicon having the diamond

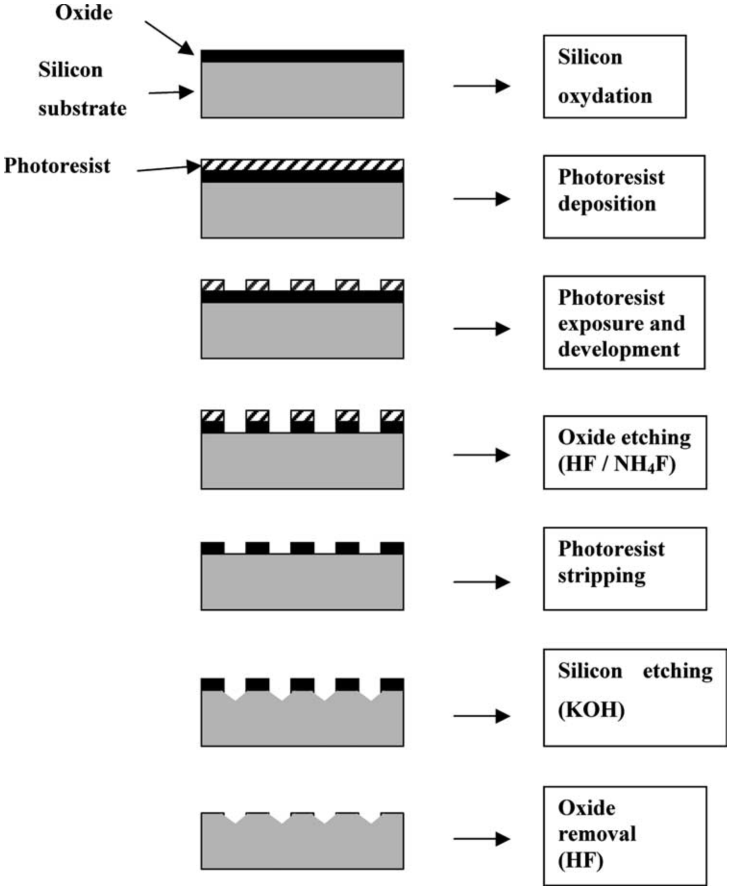

Fig. 3. Steps of the grating fabrication process.

structure, etching is faster along some crystallographic planes than along other stable planes [21]. Specific shapes or structures as V-grooves, pyramidal tips and pyramidal cavities are often obtained in silicon. An etchant that exhibits such orientation-dependent etching properties in silicon consists of a mixture of KOH and isopropyl alcohol [22].

3.2. Experimental procedures

The grating fabrication process is shown in Fig. 3. The investigated samples were boron-doped p-type {1 0 0} oriented Czochralski silicon wafers. A 500-nm-thick thermal oxide is grown by a wet oxidation of the substrate. Then, a classical positive photoresist (Shypley S1805) is deposited by spin-coating at 4000 rpm, and softbaked at 95 °C. Samples are then exposed to UV-light at 365 nm for pattern transfer from the photolithography mask (array of squares) to the photoresist. After a development stage, the samples are hard-baked at 120 °C in order to harden the photoresist and prevent it from peeling or etching in solutions. The samples are then immersed in HF/NH_4F aqueous solution to etch silicon oxide zones uncovered by the photoresist. After stripping the photoresist in acetone, the samples are immersed in 35 wt% KOH solution for 3–5 min at 80 °C, depending on the etching depth desired. Finally, the silicon oxide mask is dissolved in HF in order to characterize the silicon grating.

4. Results

4.1. Etching results

Several samples have been fabricated. Among them, we show the results obtained with the one that exhibits the lowest reflectance. Fig. 4 is a Nomarsky microscope image of the grating's surface. As can be seen, a uniform pattern has been obtained. Fig. 5 shows the results given by atomic force microscopy (AFM). Fig. 5(a) shows a top view of the etched surface and the profile of the etched structures along the cross-section AA$'$. Finally, Fig. 5(b) is the 3D perspective view. Fig. 5(a) shows that, as expected by the convex-shaped silicon etching theory [23] and illustrated in Fig. 6, the grating has a pyramidal profile. The top of the pyramids exhibits a flat surface with a 1.1 μm side, which demonstrates that the protecting oxide layer was not entirely under-etched. It is also shown that the {1 1 0} oriented side-walls of the pyramids make an inclination angle of about 42° with the horizontal {1 0 0} surface. According to the Fig. 6, we expected to measure an inclination angle of 45° corresponding to {1 1 0} planes. This low deviation may be explained by the convolution of the grating's profile with the shape of the AFM tip. Finally, the etched depth obtained after 5 min etching in a 80 °C KOH solution, is 1.9 μm.

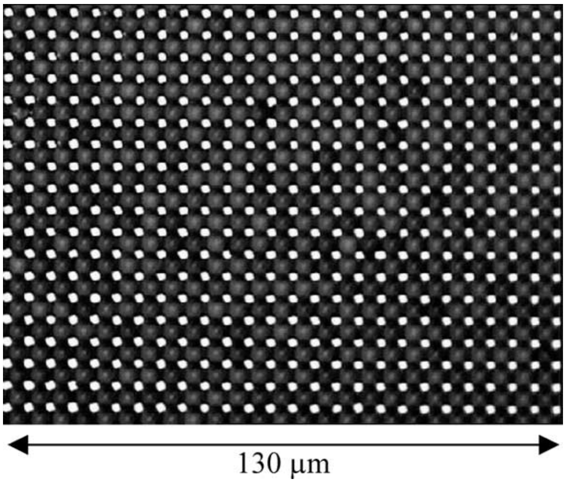

Fig. 4. Nomarsky microscope image of the sample. The pyramidal profile of the grating is represented in top view. The distance between two dots is the period $d = 5$ μm of the grating.

4.2. Optical properties

The reflectance in normal incidence of the corrugated surface has been measured by infrared (IR) spectrophotometry. Fig. 7 shows the corresponding experimental results. It can be noticed that a strong broadband antireflection effect is obtained (the reflectance is less than 2.5% in the whole spectral region). The measured reflectance is smaller than what predicted by the modal method (see Fig. 2). This discrepancy is due to the particular profile of the etched grating (see Fig. 5(a)). In

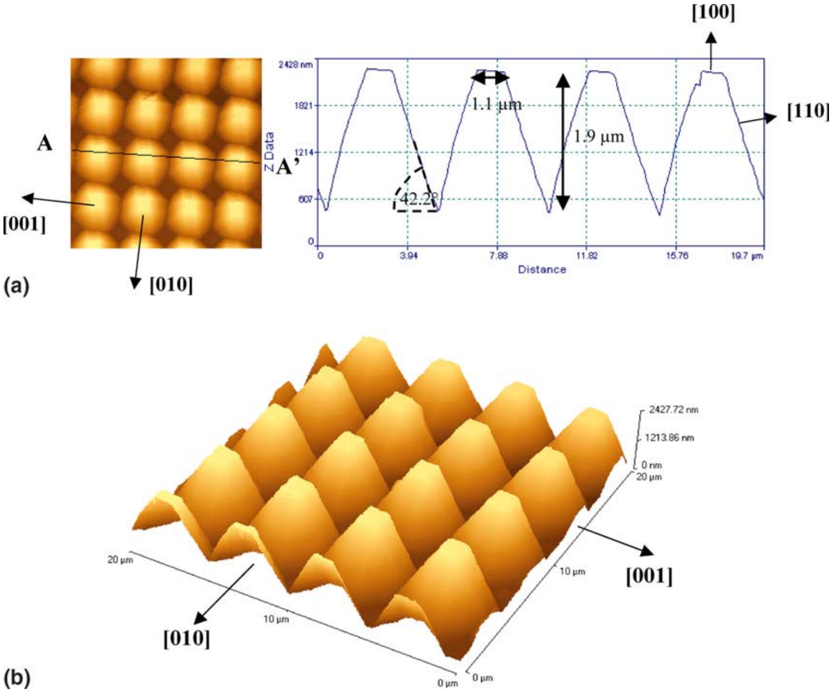

Fig. 5. AFM images of the grating. The orientation of the {1 0 0}, {0 1 0} and {1 1 0} planes are represented. Period $d = 5$ µm. (a) Left: top view; right: profile along cross section AA$'$. (b) 3D perspective view.

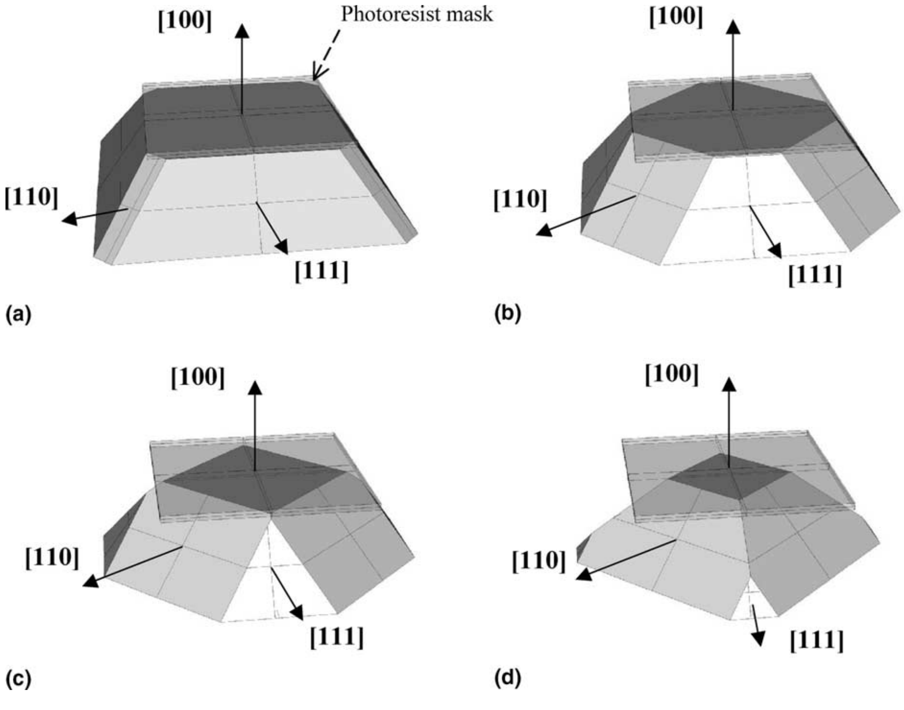

Fig. 6. Silicon etching evolution with a convex-shaped mask.

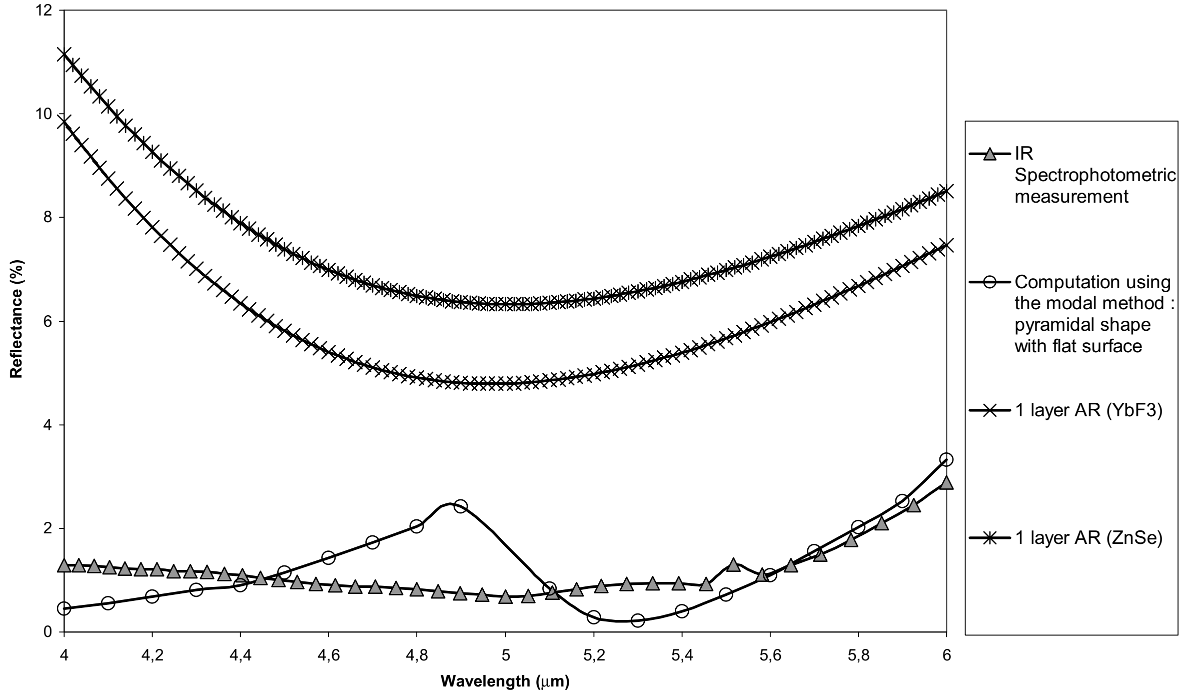

Fig. 7. Comparison between numerical simulation and experimental results. The reflectance obtained with two different standard low-index coatings is also presented.

order to explain the experimental result, we have computed the reflectance of the sample by using a rigorous modal method where the profile of the corrugated surface (with a flat surface on the top of the pyramids) measured by AFM was taken into account. A good agreement was obtained between the numerical results and the experimental ones (Fig. 7). A slight disagreement can be noticed around 5 μm, which corresponds to the Rayleigh anomaly for $[1,0]$, $[0,1]$, $[-1,0]$ and $[0,-1]$ reflected orders. Around this region, the amount of reflected light is strongly dependent on the grating's profile. The presence of sidewalls corresponding to under-etched $\{1\,1\,1\}$ planes (see Fig. 6), that are difficult to see on AFM images, could lead to a particular profile that is not taken into account in the calculation. Moreover the incident beam in the spectrophotometer, used to illuminate the grating, has an angular aperture of 4° while the theoretical calculation is made with a incident plane wave. Then, the measured reflectance is the result of a convolution between the incident beam and the angular dependence of the efficiency of the reflected zero order. This could lead to a "smoothing effect" in the measured reflectance curve which does not exhibit the "kink" obtained around 5 μm for the theoretical curve. Concerning the transmitted light, as the refractive index of silicon n_{Si} was taken equal to 3.42 with the imaginary part equal to 0, the amount of transmitted light T is equal to $1 - R$ where R is the reflected energy. In particular, with this structure, T is around 97.5% and the efficiency in the zeroth reflected order is lower than 5.3% in the whole spectral region. Calculations for incidence angles up to 5° show that the reflected intensity in the zero order remains smaller than 6% in the whole spectral region for both polarization states. This result shows that the antireflection grating is compatible with the use of slightly divergent incident beams. This property shows that the grating can be used for stealth applications in the infrared spectral region.

For comparison purposes, the spectral reflectance of two different single-layer antireflective coatings deposited on a silicon substrate have been computed; they are presented in Fig. 7. We considered two coatings made from low-index materials (YbF_3 and ZnSe) commonly used in the infrared ($n_{YbF3} = 1.49$ and $n_{ZnSe} = 2.43$). The reflectance of the antireflective silicon grating is much lower than that of the single-layer antireflection coatings in the whole measured spectral range. A lower reflectance could be obtained with multilayer coatings; however, the thickness of such coatings, which is typically greater than 5 μm, can lead to problems of surface adhesion or to losses of energy due to absorption. This clearly emphasizes the interest of a corrugated surface.

5. Conclusion

We have shown that the reflectance of silicon wafers can be strongly reduced in normal incidence with pyramid-shaped gratings by a factor greater than 10, even when the period is close to the wavelength of illumination. A wet etching technique of silicon has been used to fabricate a grating that was characterized by a standard IR spectrophotometric technique and by atomic force microscopy. A good agreement between experimental results and theoretical ones has been obtained. These results have shown that a slight modification of the profile predicted by the effective medium theory leads to better antireflection properties of the grating. A reflectance around 2% in the whole [4μm; 6μm] spectral range has been obtained without using high resolution etching techniques.

Acknowledgements

The authors thank Dr. S. Enoch for the calculations using the modal method, Dr. F. Lemarquis for IR spectrophotometric measurements, Z. Elalamy for 3D etching drawings and Prof. T. Kakouridis for improving the English. This research has been partially funded by Region Provence Alpes Côte d'Azur (Grants 00/1548700 and 00/1548900), Conseil Général des Bouches-du-Rhône, The European Fund for Regional Economic Development (FEDER – Grant 823) and The Social European Fund (FSE – Grant 2002.21.02/0010).

References

[1] S.J. Wilson, M.C. Hutley, Opt. Acta 29 (1982) 993.
[2] D.H. Raguin, G.M. Morris, Appl. Opt. 32 (1993) 113.
[3] P. Lalanne, G.M. Morris, Nanotechnology (Bristol) 8 (1997) 53.
[4] P. Sheng, A.N. Bloch, R.S. Stepleman, Appl. Phys. Lett. 43 (1983) 579.
[5] N.F. Hartman, T.K. Gaylord, Appl. Opt. 27 (1998) 3738.
[6] R.C. Enger, S.K. Case, Appl. Opt. 22 (1983) 3220.
[7] T.K. Gaylord, E.N. Glytsis, M.G. Moharam, Appl. Opt. 26 (1987) 3124.
[8] G. Bouchitté, R. Petit, Electromagnetics 5 (1985) 17.
[9] E.B. Grann, M.G. Moharam, D.A. Pommet, J. Opt. Soc. Am. A 13 (1995) 333.
[10] W.H. Southwell, J. Opt. Soc. Am. A 8 (1991) 549.
[11] L. Li, J. Opt. Soc. Am. A 14 (1997) 2758.
[12] W.A. Kern, C.A. Deckert, in: J.L. Vossen, W. Kern (Eds.), Thin Film Processes, Academic Press, New York, 1978, p. 401.
[13] W. Tsang, S. Wang, J. Appl. Phys. 46 (1975) 2163.
[14] Y. Fujii, IEEE J. Quantum Electron. QE-16 (1980) 165.
[15] J.C. Greenwood, in: R.A. Levy (Ed.), Novel Silicon Based Technologies, Kluwer Academic, Dordrecht, 1991, p. 123.
[16] U.U. Graf, D.T. Jaffe, E. Kim, J.H. Lacy, H. Ling, J.T. Moore, G. Rebeiz, Appl. Opt. 33 (1994) 96.
[17] G. Wiedemann, D.E. Jennings, Appl. Opt. 32 (1993) 1176.
[18] P.J. Kuzmenko, D.R. Ciarlo, C.D. Stevens, in: J. Wang, P.B. Hays (Eds.), Optical Spectroscopic Techniques and Instrumentation for Atmospheric and Space Research, Proc. SPIE, 2266, 1994, p. 566.
[19] P.J. Kuzmenko, D.R. Ciarlo, in: A.M. Fowler (Ed.), Infrared Astronomical Instrumentation, Proc. SPIE, 3354, 1998, p. 357.
[20] F. Nikolajeff, B. Löfving, M. Johansson, J. Bengtsson, S. Hard, C. Heine, Appl. Opt. 39 (2000) 4842.
[21] K.E. Bean, IEEE Trans. Electron. Devices ED-25 (1978) 1185.
[22] Y. Kanamori, M. Sasaki, K. Hane, Opt. Lett. 24 (1999) 1422.
[23] M. Shikida, K. Nanbara, T. Koizumi, H. Sasaki, M. Odagaki, K. Sato, M. Ando, S. Furuta, K. Asaumi, Sensors Actuators A 97–98 (2002) 758.